Polar Biol
DOI 10.1007/s00300-015-1842-5

ORIGINAL PAPER

# The taxonomic challenge posed by the Antarctic echinoids *Abatus bidens* and *Abatus cavernosus* (Schizasteridae, Echinoidea)

**Bruno David[1,4] · Thomas Saucède[1] · Anne Chenuil[2] · Emilie Steimetz[1] · Chantal De Ridder[3]**

Received: 31 August 2015 / Revised: 6 November 2015 / Accepted: 16 November 2015


**Abstract** Cryptic species have been repeatedly described for two decades among the Antarctic fauna, challenging the classic model of Antarctic species with circumpolar distributions and leading to revisit the richness of the Antarctic fauna. No cryptic species had been so far recorded among Antarctic echinoids, which are, however, relatively well diversified in the Southern Ocean. The R/V *Polarstern* cruise PS81 (ANT XXIX/3) came across populations of *Abatus bidens*, a schizasterid so far known by few specimens that were found living in sympatry with the species *Abatus cavernosus*. The species *A. cavernosus* is reported to have a circum-Antarctic distribution, while *A. bidens* is only recorded with certainty in South Georgia and at the northern tip of the Antarctic Peninsula. Based on genetic and morphological analyses, our results clearly show that *A. bidens* and *A. cavernosus* are two distinct species. The analyzed specimens of *A. bidens* group together in two haplogroups separated from one another by 2.7 % of nucleotide differences. They are located in the Weddell Sea and in the Bransfield Strait. Specimens of *A. cavernosus* form one single haplogroup separated from haplogroups of *A. bidens* by 5 and 3.5 % of nucleotide differences, respectively. The species was collected in the Drake Passage and in the Bransfield Strait. Morphological analyses differentiate *A. bidens* from *A. cavernosus*. In contrast, the two genetic groups of *A. bidens* cannot be differentiated from one another based on morphology alone, suggesting that they may represent a case of cryptic species, common in many Antarctic taxa, but not yet reported in Antarctic echinoids. This needs to be confirmed by complementary analyses of independent genetic markers.

**Keywords** *Abatus bidens* · *Abatus cavernosus* · Cryptic species · Echinoidea · Schizasteridae · Southern Ocean

This article belongs to the special issue on "High environmental variability and steep biological gradients in the waters off the northern Antarctic Peninsula," coordinated by Julian Gutt, Bruno David, and Enrique Isla

✉ Thomas Saucède
thomas.saucede@u-bourgogne.fr

[1] UMR6282 Biogéosciences, CNRS - Université de Bourgogne Franche-Comté, 6 boulevard Gabriel, 21000 Dijon, France

[2] Institut Méditerranéen de Biodiversité et d'Ecologie marine et continentale, UMR CNRS 7263, Aix-Marseille Université, IRD, Station Marine d'Endoume, Chemin de la Batterie des Lions, 13007 Marseille, France

[3] Laboratoire de Biologie Marine (CP 160/15), Université Libre de Bruxelles, 50 Avenue F.D. Roosevelt, 1050 Brussels, Belgium

[4] Muséum National d'Histoire naturelle, 57 rue Cuvier, 75005 Paris, France

## Introduction

For two decades, cryptic species have been repeatedly described among the Antarctic fauna, challenging the former, classic biogeographic model of Antarctic species with wide, circumpolar distributions (De Broyer et al. 2011; Dettai et al. 2011). The richness and spatial distribution of the Antarctic fauna have been revisited and the underpinning evolutionary processes re-assessed (Kaiser et al. 2013). The occurrence of cryptic species in the Southern Ocean and on the Antarctic continental shelf in particular was highlighted in many studies of population genetics, in some cases even signing the existence of species flocks (Lecointre et al. 2013). Cryptic species have been described in various Antarctic groups: polychaetes (Schüller

Published online: 01 December 2015

2011), gastropods (Wilson et al. 2013), bivalves (Linse et al. 2007), crustaceans (Held and Wägele 2005; Raupach and Wägele 2006), pycnogonids (Krabbe et al. 2009), cephalopods (Allcock et al. 2010), crinoids (Wilson et al. 2007; Hemery et al. 2012), holothuroids (O'Loughlin et al. 2011), and fish (Smith et al. 2011). Whatever the clade considered, depending on historical and environmental contingencies, the processes leading to cryptic speciation can be related to spatial isolation, disruptive selection, and ecological divergence. Cryptic species being recurrently described in various Antarctic clades, theirs origins must be soughed for in mechanisms impacting the entire Antarctic fauna and linked to relatively fast landscape dynamics, that is rapid alternation between allopatry and sympatry (Aguilée et al. 2012). A common explanation resides in the alternation between glacial and interglacial periods that forces populations to isolated, glacial refugia or otherwise allows spatial range expansion (Thatje et al. 2005; Allcock and Strugnell 2012; Aguilée et al. 2012).

Unexpectedly, no cryptic species had been so far recorded among Antarctic echinoids, which are, however, relatively well diversified in the Southern Ocean (Saucède et al. 2014). Spatangoid irregular echinoids in particular form the most speciose group of echinoids in the Southern Ocean. It is exclusively represented there by the family Schizasteridae and counts 30 morphologically recognized species and eight genera (David et al. 2005a, b; Pierrat et al. 2012; Saucède et al. 2014). Most species are brooders, the females incubating their young in deepened petals that form kinds of pouches or marsupia. Such a life history trait implies limited dispersal capabilities that might have facilitated this outstanding diversification of the group also promoted by the alternation between glacial and interglacial periods and the Antarctic Circumpolar Current (Poulin et al. 2002; Pearse et al. 2009). All Antarctic species of Schizasteridae constitute a single monophyletic group, which presumably represents a species "core flock" (sensu Lecointre et al. 2013) endemic to the Antarctic continental shelf including its deepest parts (David et al. 2005a; Pearse et al. 2009; Lecointre et al. 2013; Saucède et al. 2014). Schizasterids are deposit feeders and soft-bottom dwellers, and they live more or less buried into the superficial sediment layer.

The systematics of Antarctic Schizasteridae has long been explored based on morphological observations (e.g., Mortensen 1909, 1910; Koehler 1912; Pawson 1969; David et al. 2005a, b for the most recent reviews), but several species are known by few specimens and still remain poorly described. Considering the significant variation of morphological characters such as test outline and plating, development and position of fasciolar bands and of other appendages, the taxonomy of Antarctic Schizasteridae and the phylogenetic relationships among species remain puzzling, pending for new appraisals grounded on molecular markers. The R/V *Polarstern* cruise PS81–ANT XXIX/3 (Gutt 2013) came across populations of *Abatus bidens*, a schizasterid so far known by few specimens that were found living in sympatry with the species *Abatus cavernosus*. The species were formerly considered as two varieties of a same species (Mortensen 1951) before they were placed in two distinct entities (David et al. 2005a). The species *A. cavernosus* is so far reported to have a circum-Antarctic distribution, while *A. bidens* is only recorded with certainty in South Georgia and at the northern tip of the Antarctic Peninsula. The latter species was also reported in Adelie Land where its occurrence remains uncertain (David et al. 2005a). The present study fully describes the species *A. bidens* for the first time and assesses morphological and genetic variations between the two forms. What are the morphological and genetic differences between *A. bidens* and *A. cavernosus*? Are there reliable, genetic differences to support the distinction between the two nominal species? Are there transitional forms to suggest that they are cryptic species if any?

## Materials and methods

### Material studied

Seventy-nine specimens of *A. bidens* and *A. cavernosus* were collected at 19 stations in the northwest of the Weddell Sea, in the Bransfield Strait, and in the Drake Passage during cruise PS81 of the R/V *Polarstern* (Fig. 1; Table 1). Specimens were collected between 102 and 782 m depth using an Agassiz trawl (Gutt 2013). The two species were found in sympatry at five of the 19 stations. Specimens were subsequently fixed in 96 % ethanol and are now housed in collections of the University of Burgundy (Dijon, France). Taxonomy of Antarctic species of the family Schizasteridae is really challenging as shown for long by previous studies (David et al. 2005a, Saucède et al. 2014). We therefore concentrated our study on recently sampled specimens during cruise PS81, for which a special care was taken to control sample preservation, morphological study, and taxonomic identification. Genetic and morphometric analyses were performed independently.

### Genetic analyses

Genetic analyses initially included 62 specimens among which 49 provided informative sequences to be analyzed. Tissue samples were taken on echinoid spines, and DNA was extracted using the Chelex method following Chenuil and Féral (2003). A typical barcoding region of the

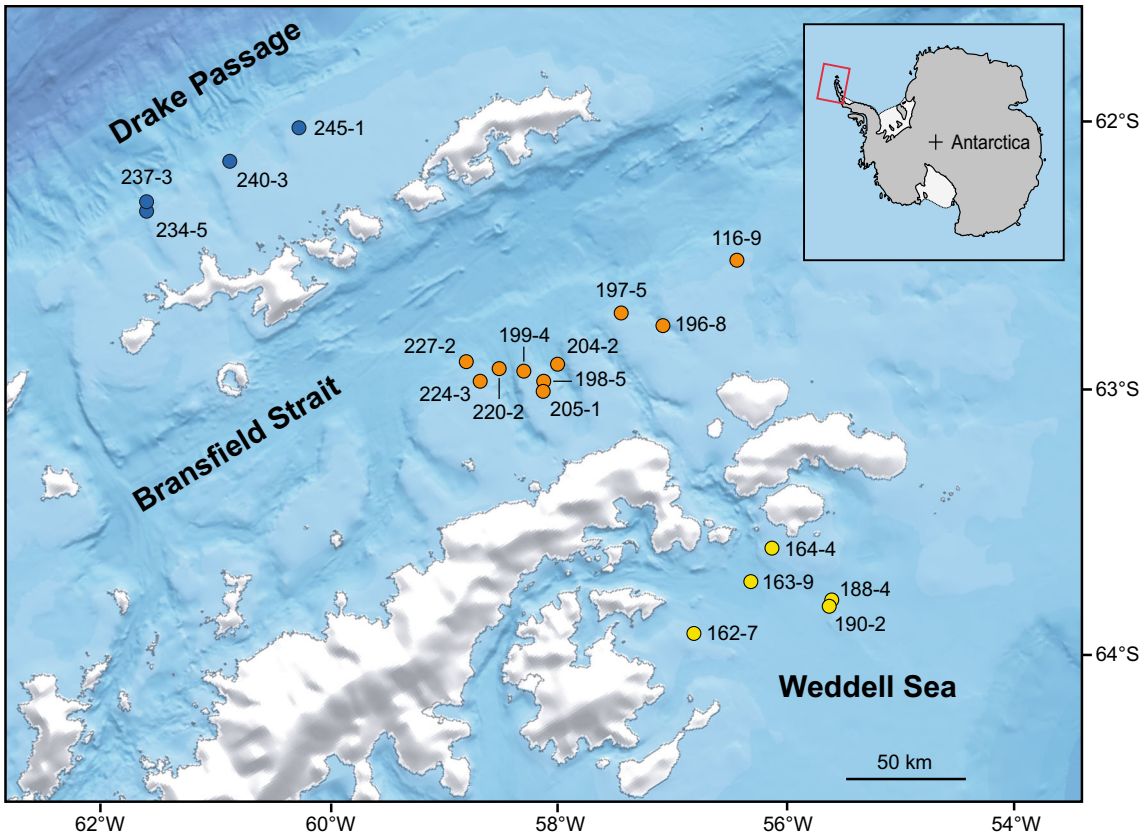


**Fig. 1** Nineteen stations in the Weddell Sea (*yellow dots*), Bransfield Strait (*orange dots*), and Drake Passage (*blue dots*) where the studied specimens of *Abatus cavernosus* and *Abatus bidens* were collected during cruise PS81 of the R/V *Polarstern*. (Color figure online)

mitochondrial cytochrome oxidase gene was amplified by PCR using the primers COIe3 (5′-GCTCGTGC(A/G)TC TAC(A/G)TCCAT-3′) and COIe5 (5′-GC(C/T)TGAGC(A/ T)GGCATGGTAGG-3′) from Stockley et al. (2005). PCR amplicons were sent to the industry (Eurofins Genomics) for Sanger sequencing. DNA sequences were manually trimmed and checked using the program Bioedit (Hall 1999). Haplotype networks were built by the median-joining method using the Network software (Bandelt et al. 1999). A color code was used to identify the morphological species, the geographical region (the Weddell Sea, the Bransfield Strait, or the Drake Passage), and the sampling stations of each haplotype owing to the NetworkPublisher software (Bandelt et al. 1999).

### Morphological analyses

Echinoids were observed under a binocular microscope, and morphology was analyzed using 10 quantitative parameters measured on echinoid tests with a digital caliper to the nearest 0.1 mm. These measurements were defined based on the morphological characters described in diagnoses of Antarctic echinoid species (David et al. 2005a). They are total test length (LL), total test width (WD), total test height (HT), distance between the apical system and the back of the test (AS), length of posterior petal I (PPT), length of anterior petal II (APT), distance between center of the apical system and beginning of petal II (DP), distance between the periproct and the base of the test (PP), distance between the peristome and the back of the test (PS), and total number of adjacent ambulacral plates abuting the labrum (LB) (Fig. 2). Echinoid size was estimated using the geometric mean of test length, width, and height (i.e., the cube root of their product), and test shape (i.e., test proportions) was analyzed using seven indices computed from ratios between some of the 10 measured quantitative parameters: shape at the ambitus (AMB = WD/LL), gibbosity (GIB = HT/[$\sqrt{}$(LL.WD)]), relative position of the peristome (RPS = PS/LL), relative position of the periproct (RPP = PP/HT), relative position of the apical system (RAS = AS/LL), relative size of the petals (RPET = PPT/APT), relative importance of the gap between the apical system and the beginning of petal II (RDP = DP/APT). Morphometric analyses were performed on 75 specimens, 57 identified as *A. bidens* and 18 as *A. cavernosus*, using the softwares Past (Hammer et al.

**Table 1** Sites where specimens of the species complex *Abatus cavernosus–Abatus bidens* were collected. Crosses indicate where the haplogroups were formally identified and where non-sequenced specimens were identified based on morphology alone

| Sampling sites | *Abatus bidens* | | | *Abatus cavernosus* | |
|---|---|---|---|---|---|
| | Haplogroup G1 | Haplogroup G2 | Non-sequenced | Haplogroup G3 | Non-sequenced |
| Weddell (162-7) | | X | | | |
| Weddell (163-9) | X | X | | | X |
| Weddell (164-4) | X | X | | | X |
| Weddell (188-4) | | | X | | |
| Weddell (190-2) | | | X | | |
| Bransfield (116-9) | | | | X | |
| Bransfield (196-8) | | | X | | |
| Bransfield (197-5) | X | | | | |
| Bransfield (198-5) | | X | | | X |
| Bransfield (199-4) | | | X | | |
| Bransfield (204-2) | X | X | | | |
| Bransfield (205-1) | | | X | | |
| Bransfield (220-2) | X | X | | X | |
| Bransfield (224-3) | X | X | | X | |
| Bransfield (227-2) | X | | | | |
| Drake (234-5) | | | | X | |
| Drake (237-3) | | | | | X |
| Drake (240-3) | | | | | X |
| Drake (245-1) | | | | | X |

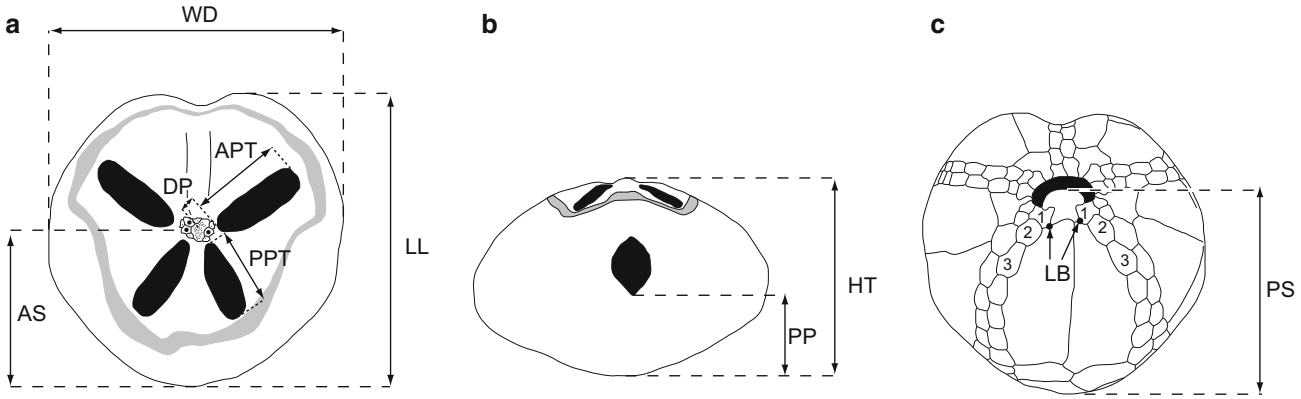


**Fig. 2** Measurements taken in the morphometric analysis. **a** Echinoid test drawn in apical view (fasciolar band in *light gray*, brood pouches in *black*, apical system detailed in the *center*). **b** Test in posterior view (fasciolar band in *light gray*, brood pouches and periproct in *black*). **c** Test in oral view with details of plate patterns (peristome in *black*). **a** Total test length (LL) and width (WD), distance between the apical system and the back of the test (AS), length of posterior petal I (PPT), length of anterior petal II (APT), distance between center of the apical system and beginning of petal (pouch) II (DP). **b** Total test height (HT), distance between the periproct and the base of the test (PP). **c** Distance between the peristome and the back of the test (PS); total number of adjacent ambulacral plates abuting the labrum (LB). A maximum of six ambulacral plates (3 per ambulacrum) can abut the labrum in *Abatus bidens*; two ambulacral plates only abut the labrum in the specimen shown in Fig. 2c

2001) and Statistica 6.1 (Statsoft 2002). Principal component analyses (PCAs) were performed independently on the 10 quantitative parameters and on the seven indices to analyze morphological variations within and between the two species. Correlation matrices were used to compute the PCAs as raw data show contrasting units and range variations. Morphological differentiation between the two species was analyzed using discriminant analyses based on

quantitative measurements and on the indices independently. A priori groups were determined based on genetic data (see below). These analyses were complemented by parametric tests as homoscedasticity assumptions are respected (only parameters PP and LB and indices RPS and RPP show significantly different variances between the two species).

Appendages were prepared and examined following David and Mooi (1990). Pedicellariae were removed from tests and placed into 96 % ethanol. They were bleached with a 10 % solution of sodium hypochlorite to remove soft tissue and to separate the valves. Then, they were washed in water, dried for 24 h, and mounted on SEM stubs. Details of pedicellariae were examined with a tabletop scanning electron microscope, and digital images were recorded.

## Results

### Genetic analyses

After trimming, the alignment file contained 633 homologous base pairs for 49 individuals. Seven haplotypes were identified and formed three divergent haplogroups, each group including two or three haplotypes (Fig. 3). Haplogroups G1 (26 specimens) and G2 (18 specimens) were composed of specimens of *A. bidens* and were separated from one another by a minimum of 17 mutations (i.e., 2.7 % of genetic difference). The third haplogroup G3 (5 specimens) was composed of specimens of *A. cavernosus* only and was separated from haplogroups G1 and G2 by a minimum of 31 and 23 mutations, respectively (i.e., 5 and 3.5 % of genetic difference) (Fig. 3a). Haplogroups were identified at 11 of the 19 sampling stations. Haplogroup G3 was identified at stations of the Drake Passage and of the Bransfield Strait, while the two divergent haplogroups of *A. bidens* were found at stations of the Weddell Sea and of the Bransfield Strait (Fig. 3b). The three haplogroups occured in sympatry at two stations only (Sts. 220-2 and 224-3), the two haplogroups of *A. bidens*, G1 and G2, co-occurred in 3 other stations (Sts. 164-4, 204-2, and 227-2), and one single haplotype was identified at the six remaining stations (Fig. 3c).

### Morphological analyses

Within the 75 specimens measured, 41 were identified as *A. bidens* by genetic analyses, 26 belong to haplogroup G1 and 15 belong to haplogroup G2, and 5 more specimens were identified as *A. cavernosus* and belong to haplogroup G3. A total of 29 specimens could not be analyzed for genetics and were finally attributed to their respective species based on morphological results, that is 16 specimens to *A. bidens* and 13 to *A. cavernosus*. The distribution of specimens is detailed in Table 1.

Statistical analyses of morphological data clearly differentiate the two morphological species *A. bidens* and *A. cavernosus.* Five parameters, in particular, were significantly different between the two species (Student's bilateral tests are detailed in Table 2): the distance between the peristome and the back of the test (PS), the distance between the apical system and the back of the test (AS), the length of the posterior petal I (PPT), the distance between the center of the apical system and the beginning of petal II (DP), and the total number of adjacent ambulacral plates abuting the labrum (LB). Size was not significantly different between the two species (bilateral $t$ test under homoscedasticity $p = 0.47$) so that morphological differences between species are not due to allometry. Sexual dimorphism was not significant for shape (Hotelling's T-squared $p = 0.19$ and $p = 0.29$ for raw parameters and shape indices, respectively). However, size differed between females and males, females being larger than males (unilateral $t$ test $p = 0.014$, mean size of females and males 38.5 and 35.4 mm, respectively).

The principal component analysis performed on the ten quantitative parameters (Fig. 4) shows that the two species mainly differentiate from one another along PC2 (14.2 % of the total variance), which is mainly due to three parameters: labrum extension (LB), length of posterior petal I (PPT), and position of the apical system (AS). The principal component analysis performed on shape indices gave congruent results with a clear differentiation of the two species along the two first PCs (62.9 % of the total variance). Differentiation mainly implies three indices: the shape of the ambitus (AMB), the relative position of the apical system (RAS), and the posterior/anterior ratio between petals (RPET). Congruent results of the two PCAs show that specimens of *A. bidens* have a more extended labrum, a more elongated ambitus, a more anterior apical system, and a longer posterior petal than specimens of *A. cavernosus*. This morphological difference is also supported by the discriminant analyses performed on raw parameters and shape indices, with a high attribution ratio of 98.7 % for both parameters and indices (Hotelling's T-squared $p = 9.3 \times 10^{-15}$ and $p = 2.3 \times 10^{-19}$, respectively).

Morphological variations between the two genetic groups of *A. bidens*, G1 and G2, were also analyzed. No conspicuous difference was noticed between the two groups when specimens were observed at the naked eye and under the binocular microscope, but statistical analyses revealed significant differences for the three following parameters: test height (HT), labrum extension (LB), and

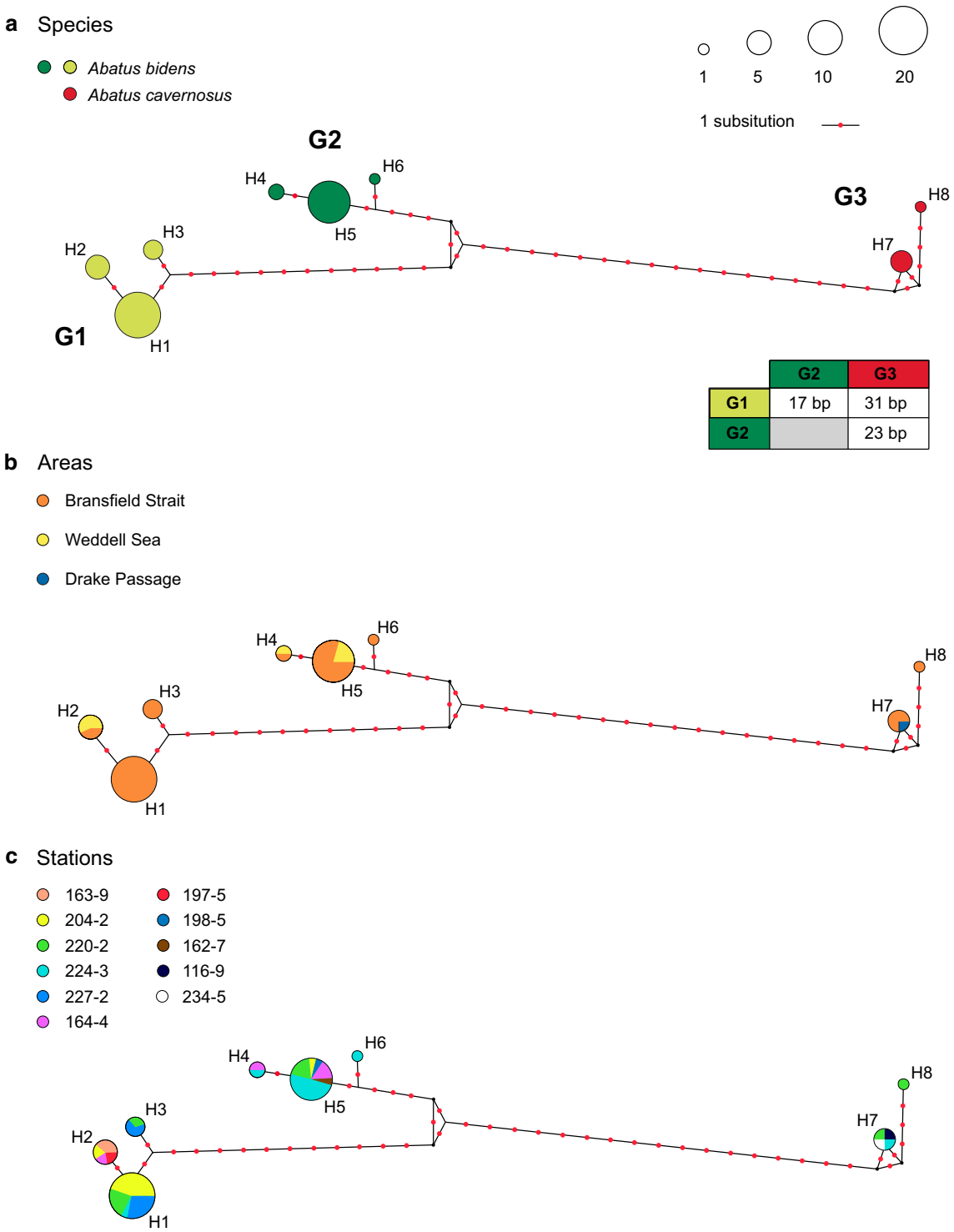


**Fig. 3** Median-joining network of haplotypes based on mtDNA COI sequences obtained from 5 specimens of *Abatus cavernosus* and 44 specimens of *Abatus bidens*. **a** Each haplotype is labelled from H1 to H8 and shown in a *colored circle* indicating the genetic unit to which it belongs: G1 (*light green*), G2 (*dark green*), and G3 (*red*). Size of circles are proportional to frequency in the sample analyzed. Mutations are shown with *unlabelled red dots*. Minimum pairwise distances (minimum number of mutations) between specimens of the three groups are shown in the table inserted. **b** *Colors* indicate the sampling region of each haplotype: the Bransfield Strait (*orange*), Weddell Sea (*yellow*), and Drake Passage (*blue*). **c** *Colors* indicate the sampling station of each haplotype. (Color figure online)

**Table 2** Morphological differences between haplogroups of *Abatus bidens* and *Abatus cavernosus*

| Parameters | LL, WD, HT, PP, APT | PS | AS | PPT | DP | LB |
|---|---|---|---|---|---|---|
| *p* values | >0.05 | 0.004 | $1.6 \times 10^{-7}$ | $1.2 \times 10^{-9}$ | 0.015 | $1.3 \times 10^{-6}$ |

The table gives the probability values for Student's bilateral tests. Significant values only are detailed (abbreviations are given in Fig. 2)

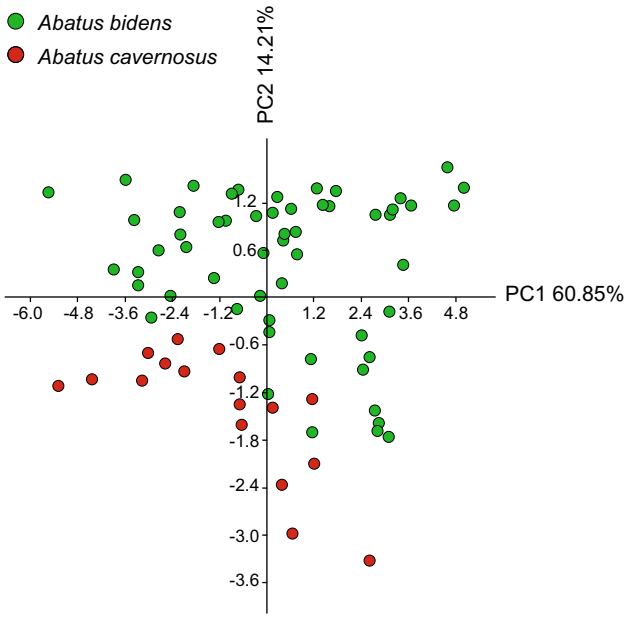


**Fig. 4** Principal component analysis of the ten raw morphometric parameters measured in specimens of *Abatus bidens* (*green dots*) and *Abatus cavernosus* (*red dots*). The two species differentiate along the first two principal components, which account for 75.06 % of the total variance. (Color figure online)

**Table 3** Morphological differences between haplogroups G1 and G2 of *Abatus bidens*

| Parameters | LL, WD, PS, PP, AS, PPT, APT | HT | DP | LB |
|---|---|---|---|---|
| *p* values | >0.05 | 0.02 | 0.01 | 0.01 |

The table gives the probability values for Student's bilateral tests. Significant values only are detailed (abbreviations are given in Fig. 2)

distance between the apical system and the beginning of petal II (DP) (Table 3). Variation ranges, however, widely overlap, and clear, diagnostic morphological characters cannot be identified to differentiate the two groups. These results are also supported by the PCAs performed on raw parameters (Fig. 5) and shape indices independently. The PCA of raw parameters shows no clear differentiation between morphologies of the two groups along the first two PCs (Fig. 5a), the two groups best differentiating along PC3, which only accounts for 9.35 % of the total variance, though widely overlapping with one another (Fig. 5b). These results are congruent with those of the discriminant analyses (Hotelling's T-squared $p = 1.6 \times 10^{-5}$ and $p = 0.005$ for raw parameters and shape indices, respectively), the two groups best differentiating for raw parameters. This discriminant analysis performed on raw parameters also shows that the two groups of *A. bidens* partly overlap with one another in morphology but clearly differentiate from *A. cavernosus* (Fig. 6).

The three haplogroups all differ significantly from each other in some of the measured, raw morphological parameters. Pairwise Mahalanobis distances between the three groups were all tested significant regarding raw parameters, while for shape indices, only the Mahalanobis distance between G1 and G2 is not significant (Table 4). Haplogroup G1 turns out to be the most different from G3 in morphology, while G2 is intermediate in position. This totally agrees with genetic results, the distance between G1 and G3 being the longest as well (Fig. 3a).

Besides morphometric analyses, qualitative characters were also examined to complement the morphological study, including observation of appendages (Table 5; Fig. 7). Some characters appear clearly diagnostic of *A. cavernosus* and differentiate it from *A. bidens*. In contrast, no single character differentiates the two groups of *A. bidens* from one another.

The test outline is heart-shaped in *A. cavernosus*, and it is angular with a truncated posterior end in *A. bidens*. The width/length ratio is significantly different between the two species, *A. bidens* being the most elongated (unilateral t test on AMB $p = 2.16 \times 10^{-6}$). All petals are almost of the same size in *A. bidens* (mean posterior petals size reaches 93 % of that of anterior ones), while posterior petals are shorter in *A. cavernosus* (mean ratio = 64 %). The color of test and spines is light brown in *A. bidens*, darker in *A. cavernosus*. The fasciolar band appears beige in *A. bidens*, in which it passes very low anteriorly, and dark purple in *A. cavernosus*. The apical system is anterior in position in *A. bidens*, centered in *A. cavernosus* (it is situated at 39 and 51 % of total test length in *A. bidens* and *A. cavernosus*, respectively).

Regarding plate patterns, in *A. cavernosus* the labrum is short and does not extend farther than the first, infrequently the second adjacent ambulacral plate, while in *A. bidens* the labrum extends as far as the third adjoining ambulacral

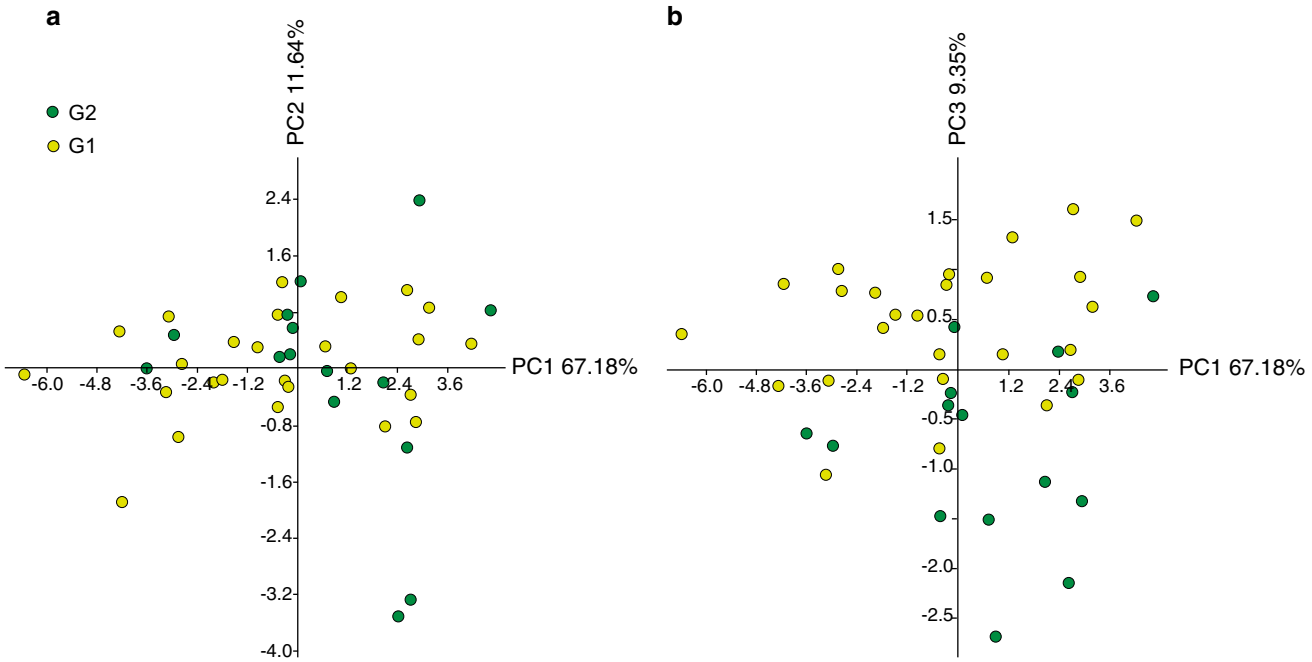


**Fig. 5** Principal component analysis of the ten raw morphometric parameters measured in specimens of *Abatus bidens* (G1, *light green dots*; G2, *dark green dots*). **a** The first two principal components, which account for 78.82 % of the total variance. **b** First and third principal components, which account for 76.53 % of the total variance. (Color figure online)

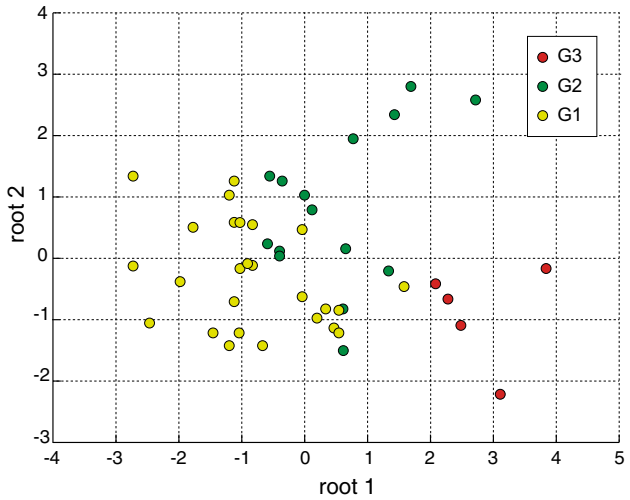


**Fig. 6** Discriminant analysis of the ten raw morphometric parameters measured in specimens of *Abatus bidens* (G1 *light green dots*; G2 *dark green dots*) and *Abatus cavernosus* (G3 *red dots*). (Color figure online)

**Table 4** Pairwise Mahalanobis distances between haplogroups G1, G2, and G3 of *Abatus bidens* and *Abatus cavernosus*, respectively

| | G1 | G2 | G3 |
|---|---|---|---|
| G1 | | 0.0368* | 0.0005** |
| G2 | 0.7518 | | 0.0292* |
| G3 | 0.0007** | 0.0064** | |

The table gives the probability values for comparisons using raw variables (matrix upper half) and shape indices (matrix lower half). Asterisks indicate whether differences are significant (*) or highly significant (**)

plate, more rarely the second and very seldom the first one. Marsupia abut the apical system in *A. cavernosus*, which is the most frequent pattern showed by Antarctic brooding schizasterids, while they often do not start before plates 8 or 9 in anterior petals of *A. bidens*, and plates 5 or 6 in the posterior ones (Fig. 8).

Pedicellariae of the two species were observed in detail (Fig. 7). Globiferous pedicellariae are drastically distinct between the two species. They are not very numerous in *A. cavernosus* and appear black in living specimens when not cleaned of their soft tissue, and valves terminate in a series of four (rarely three) sharp, tiny teeth that are rooted on the upper margin of a circular opening (Fig. 7a). In *A. bidens*, globiferous pedicellariae are extremely numerous on the apical side and they are embedded in white tissue in living specimens, which turns dark in the specimens fixed in ethanol. Valves terminate in two to three very long hooks (Fig. 7d). Rostrate pedicellariae of the two species are relatively similar in shape except for the presence of a narrow, spiky distal tip in *A. bidens* (Fig. 7f), while it is blunt and serrated in *A. cavernosus* (Fig. 7b). Tridentate pedicellariae belong to two main types: (1) the classic type with a spoon-shaped distal part that tappers progressively

**Table 5** Diagnostic morphological characters of *Abatus bidens* (including the two genetic groups) that clearly differ from those of *Abatus cavernosus*

| | *A. bidens* | *A. cavernosus* |
|---|---|---|
| Globiferous pedicellariae | They are numerous, particularly on the apical side. Their valves terminate by two long hooks located above a narrow, elongated aperture | They are rare. When present, a series of three to four teeth borders the upper rim of a rounded aperture |
| Petals | Posterior petals about the same length as the anterior ones | Posterior petals shorter than the anterior ones |
| Color | Living specimens yellow. Globiferous pedicellaria whitish | Living specimens brownish |
| Apical system and fasciole | Shifted anteriorly | Centered |
| Labrum | It extends posteriorly to the second or third adjacent ambulacral plates | It extends posteriorly to the first (or second) adjacent ambulacral plates |
| Brooding pouches (in females) | They often start away from the apical system | Always starting close to the apical system |
| Sphaeridae | Elongated | Rounded or flattened |

Characters are listed in the order of importance for distinguishing the two species

toward the base and (2) a shovel-shaped type with the distal part separated from the base by a more or less straight shaft (Fig. 7c, e). Both types are present in the two species, but they are more elongated in *A. cavernosus* (Fig. 7c) than in *A. bidens* (Fig. 7e).

Sphaeridae are somehow rounded in *A. cavernosus* (Fig. 7g) and more elongated in *A. bidens* (Fig. 7h).

## Systematics

The systematics and taxonomy of *A. bidens* is revised below based on the new genetic and morphological results obtained in the present work. All results are congruent and show that *A. bidens* should be regarded as a distinct species, following David et al. (2005a), and not a variety (subspecies) of *A. cavernosus*, contrary to Mortensen (1951) and Kroh (2015). The description includes the two haplogroups of *A. bidens* identified in this study, G1 and G2, herein treated as two putative cryptic species. All the specimens figured and studied in the present work are housed in collections of the University of Burgundy, Dijon (France).

*Abatus bidens* Mortensen (1910)
Figures 7 and 8

*Abatus cavernosus* var. *bidens* Mortensen (1910; p. 73; Pl. 19: 32, 35, 39, 42).
*Abatus cavernosus* var. *bidens* Mortensen (1951; p. 256).
Non-*Abatus bidens* Bernasconi (1953; p. 44; Pl. 24: 1–6; Pl. 25: 1–4).
*Abatus bidens* David et al. (2005a: 190–191).
*Abatus cavernosus bidens* Kroh (2015: http://www.marinespecies.org/aphia.php?p=taxdetails&id=513701)
*Abatus bidens* Kroh (2015: http://www.marinespecies.org/aphia.php?p=taxdetails&id=160761)

Material See Table 1 for location of material examined.

Diagnosis (Table 5) Apical system anterior in position. Anterior and posterior petals of equal length. Anterior branch of the fasciole low on the test. Labrum extending posteriorly to the second or third adjacent ambulacral plate. Globiferous pedicellariae very numerous on the apical side, particularly between petals and on the two margins of the anterior ambulacrum, with valves terminating in two or three long hooks positioned at the end of a narrow, elongated aperture (Fig. 7d). Living specimens yellow with whitish globiferous pedicellariae.

### *Description*

*General morphology and plate pattern: Size* The mean length of adult specimens is 46.7 mm, the females being slightly larger than males (unilateral t test $p = 0.008$).

*Color* Living specimens beige to light brown, sometimes almost yellow (Fig. 8). The color of spines is light beige. The fasciole is of the same color, turning dark in dry specimens. Plate pattern of the apical side is more or less shown by subtle changes in coloration.

*Outline of the test* Ambitus anteriorly rounded with a faint frontal notch and somehow posteriorly truncated, making an angle covered with a tuft of spines on each side. Test width is 89–98 % of test length (94 % on average). The posterior end of the test is vertically truncated, otherwise dome-shaped. Test height is 60 % of test length. Posterior petals are slightly shorter than anterior ones and converge at a more acute angle than anterior ones.

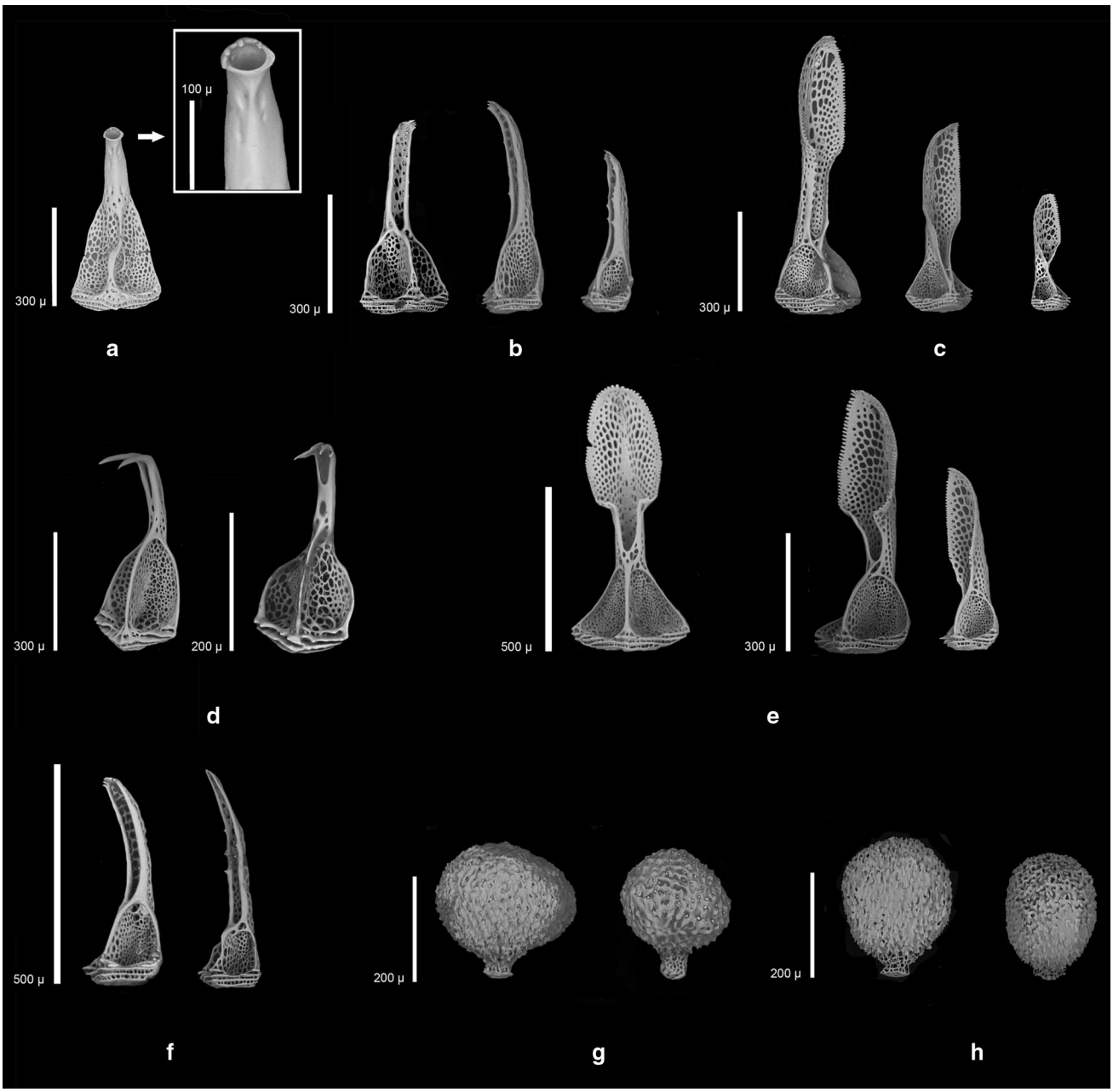


**Fig. 7** Pedicellariae and sphaeridae in *Abatus cavernosus* (**a**–**c**, **g**) and *Abatus bidens* (**d**–**f**, **h**). **a** Isolated valve of globiferous pedicellaria from specimen UBGD 279061 (G3). **b** Valves of rostrate pedicellariae from specimens UBGD 279063 (G3), UBGD 279061 (G3), and UBGD 279064 (G3) from *left* to *right*. **c** Valves of tridentate pedicellariae from specimens UBGD 279062 (G3), UBGD 279064 (G3), and UBGD 279063 (G3) from *left* to *right*. **d** Valves of globiferous pedicellariae from specimens UBGD 279067 (G1) and UBGD 279070. **e** Tridentate pedicellariae from specimen UBGD 279067 (G1). **f** Rostrate pedicellariae from specimens UBGD 279069 (G1) and UBGD 279070. **g** Sphaeridae from specimens UBGD 279062 (G3) and UBGD 279064 (G3). **h** Sphaeridae from specimens UBGD 279070 and UBGD 279068

*Apical system* It is slightly anterior in position, at 39 % of the total test length from the anterior. Plating follows the classic *Abatus* ethmolytic pattern with three gonopores (there is no gonopore in genital plate 2). Gonopores larger in females.

*Periproct* Located on the vertical posterior side, its adoral margin situated at 42 % of test height from the lower surface. It is scarcely visible in either apical or oral views. It is embedded between interambulacral plates 5.a.4/5.b.5 or 5.a.5/5.b.6 adorally, and 5.a.7/5.b.7 or 5.a.7/5.b.8 apically.

*Peristome* It is relatively large and discernible as the anterior part of the labrum does not overhang over it. It is anterior in position, located at 31 % of test length from the anterior of the test.

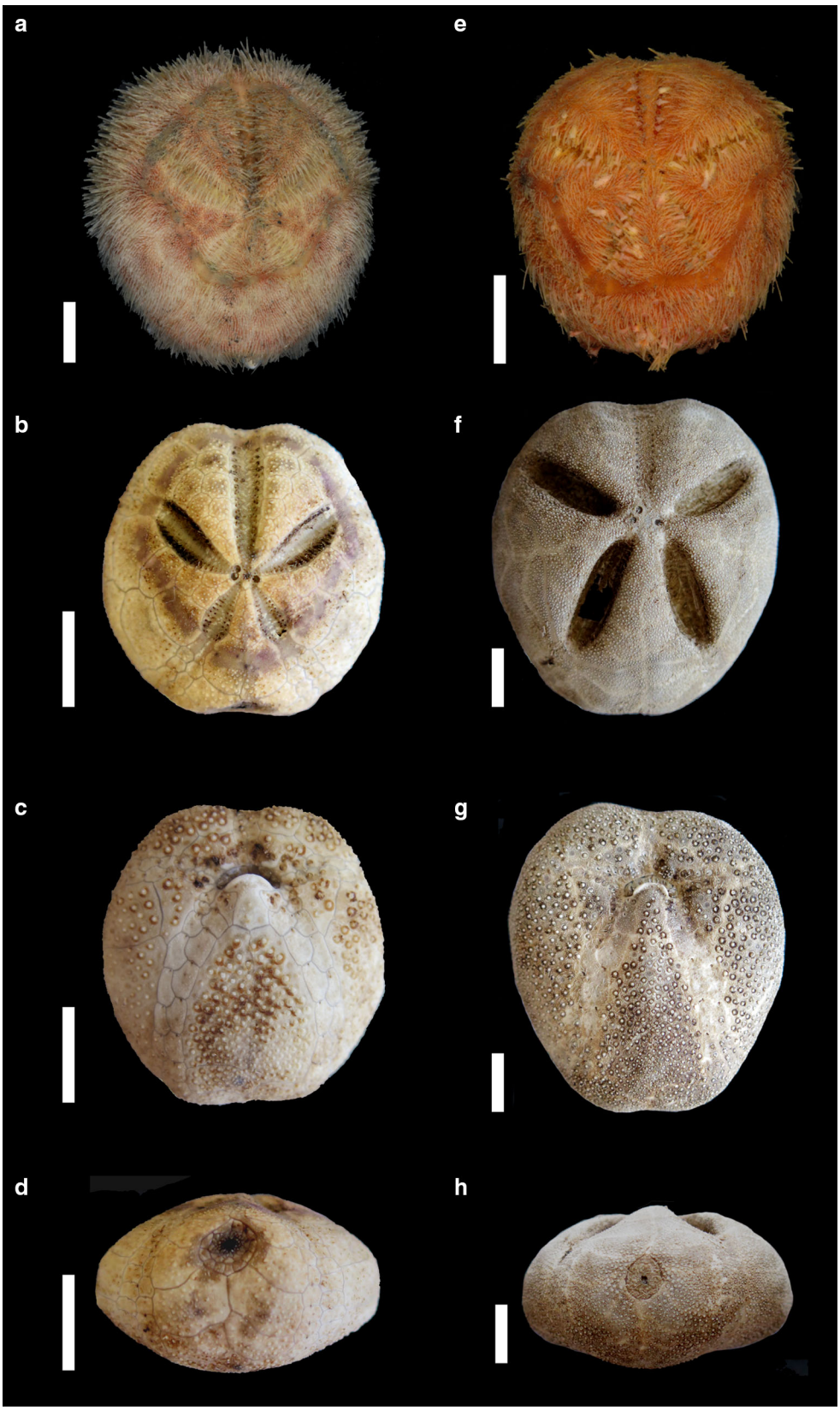


**Fig. 8** *Abatus cavernosus* (**a**–**d**) and *Abatus bidens* (**e**–**h**). **a** Apical view of fresh specimen UBGD 279059. **b** Apical, **c** oral, and **d** posterior views of denuded test of specimen UBGD 279060. **e** Apical view of fresh specimen UBGD 279065. **f** Apical, **g** oral, and **h** posterior views of denuded test of specimen UBGD 279066. *Scale bars*: 10 mm. (Color figure online)

*Plastron* In interambulacrum 5, the labrum is long, extending backward to the third or second adjacent ambulacral plates (sometimes the fourth).

Marsupiae (petals) and sexual dimorphism: Anterior and posterior petals almost of the same size, especially in haplogroup G1 (mean ratio = 0.97) compared to haplogroup G2 (mean ratio = 0.87). In most specimens, the adapical extremity of brood pouches is distant from the apical system, a morphological feature diagnostic of *A. bidens*. It is particularly conspicuous in females, in which anterior pouches initiate as far as the eighth–ninth ambulacral plates, while posterior ones are less distant from the apical system. This character is reminiscent of the plate pattern observed in *Abatus nimrodi*.

*Fasciole* The peripetalous orthofasciole (sensu Néraudeau et al. 1998) is very conspicuous and forms a broad band of 7 to over 15 rows of miliaries, depending on the segment considered and on test size. The fasciole is excentric anteriorly with the posterior segment distant from the posterior end of the test, and the anterior segment passing very close to the ambitus, barely visible in apical view.

*Appendages: Primary spines* They are relatively coarse and of the usual schizasterid shape with finely serrated longitudinal ridges. The largest spines occur on the adoral side, in the plastronal and other interambulacral areas, and are used for locomotion. Their distal extremity is gently curved. The smallest spines are on the apical side and show rounded tips.

*Secondary spines* Those observed on specimens collected at station 163-9 (Weddell Sea) are club-shaped and densely distributed.

*Miliaries* They are made of a relatively loose stereom meshwork composed of 7–8 longitudinal ridges separated by large openings. They end in a swollen serrated tip.

*Clavulae* They are straight, made of fenestrated stereom, and end in a tuft of trabeculae. They are very similar in *A. bidens* and *A. cavernosus*.

*Pedicellariae* The globiferous pedicellariae are extremely numerous, particularly on the apical side in the vicinity of petals and along each side of ambulacrum III. In living specimens, they appear as vivid yellow or whitish spots; they are brownish in specimens preserved in ethanol. Their valves terminate in two or three long hooks located at the top of an elongated opening (Fig. 7d). This character is shared with several other species of *Abatus* (e.g., *A. curvidens*, *A. agassizi*, and *A. elongatus)* and can putatively be regarded as plesiomorphic as it is also present in several species of *Amphipneustes* and *Tripylus*.

Tridentate pedicellariae (dentate pedicellariae are very commonly tridentate, sometimes bidentate) belong to two main types. As indicated above, valves of type 1 have a spoon-shaped distal part that tappers progressively toward the base (Fig. 7e). Valves of type 2 comprise three parts: the base, the intermediary tubular part, and the spoon-shaped and finely serrated distal part (Fig. 7e). Rostrate pedicellariae display a very long and curved blade with small lateral teeth along the rim of the blade (Fig. 7f).

*Sphaeridae* They are slightly ovoid and ornamented with small meridian ridges and grooves (Fig. 7h).

*Distribution*

*A. bidens* was reported with confidence by the Swedish South Polar and Discovery expeditions from the South Georgia Islands, between 64 and 270 m (Mortensen 1910), and along the Antarctic Peninsula in the Bransfield Strait and in the northwest of the Weddell Sea, between 102 and 782 m (this study).

*Remarks*

Mortensen (1951) regarded *A. bidens* as a subspecies of *A. cavernosus*, but suggested that it could be a distinct species. David et al. (2005a) considered *A. bidens* as a separate species because globiferous pedicellariae of the two species are very different. Following Mortensen (1951) and David et al. (2005a), the specimens described by Bernasconi (1953) as *A. bidens* are considered here as representatives of *Tripylus excavatus* because adult individuals possess a conspicuous latero-anal fasciolar branch, absent in *A. bidens*. The two putative cryptic species (genetic groups G1 and G2) are here referred to as *A. bidens* pending for new data.

## Discussion

In the present study, morphological and genetic results show that the two nominal species *A. cavernosus* and *A. bidens* are clearly distinct and should be regarded as truly different species as formerly suggested by David et al. (2005a). Several morphological features were recognized as clear, diagnostic characters of *A. bidens*, among which the number and shape of globiferous pedicellariae are the most remarkable (Table 5). Other distinctive and more accessible characters, albeit not so clear-cut, are petals' relative size (anterior and posterior petals are of the same size in *A. bidens*) and the position of the apical system (anterior in *A. bidens*). These characters are reliable enough for the field determination of the species.

Unexpectedly, two genetic groups of *A. bidens* were identified. The genetic divergence between the two groups (2.7 %) is significant enough to suggest that they could be reproductively isolated from each other. This is congruent

with results obtained with the molecule COI for other echinoderms. Genetic distances between closely related species of echinoderms usually range between 0.62 and 1.3 % (Ward et al. 2008; Hoareau and Boissin 2010). Some cryptic species in the same order as *Abatus*, Spatangoida, can even display up to 3 % of genetic divergence (Egea et al. 2016). For instance, the most closely related lineages within the species complex *Ophioderma longicauda* display a COI divergence of 2.2 % (Boissin et al. 2011), and cryptic species of the sand dollar *Mellita longifissa* show a genetic divergence comprised between 5.60 and 3.97 % (Coppard et al. 2013). Hence, in the present study, the 2.7 % of divergence between haplogroups G1 and G2 of *A. bidens*, the absence of intermediate forms between them, and the short genetic distance between them and *A. cavernosus* (3.5–5 %) strongly suggest that they constitute two cryptic species, all the more as schizasterid echinoids were shown to present slow rates of mitochondrial DNA evolution (Chenuil et al. 2008, 2010). Some morphological differences between the two genetic groups were tested significant, supporting, since the specimens are found in sympatry, that they may be distinct biological species, but most variations significantly overlap, justifying their qualification as cryptic. Three evolutionary scenarios, however, can challenge our interpretation because they too can generate divergent lineages within a biological species with no intermediate forms: a past demographic bottleneck, a selective sweep, and a long-lasting vicariance that did not result in an efficient reproductive barrier before "secondary" contact. The only way to rule these scenarios out and prove that haplogroups G1 and G2 form true cryptic species of *Abatus bidens*, experimental crosses excepted, would consist in characterizing at least one additional genetic marker independent from the mitochondrial COI gene, that is a DNA nuclear marker. Only the third scenario can lead to partial reproductive isolation and thus explain the significant, yet non-diagnostic, morphological differentiation observed between the two hapologroups G1 and G2.

The two groups of *A. bidens* were collected in sympatry at the scale of sampling stations (they were found together at five of the eight stations at which they were identified). *A. cavernosus* was found living in sympatry with *A. bidens* at five stations of the 12 stations at which it was collected, and the three haplogroups were found together at four of these stations. Despite the limited number of sampling sites, the occurrence of species together was frequent and attests that they can live in sympatry. The coexistence of closely related species of similar forms is generally considered a rare phenomenon as sympatry presumes the existence of differences in ecological niches and life history traits. In environments of the Southern Ocean, such cases are known in amphipods (Baird et al. 2011), isopods (Held 2001), and crinoids (Hemery et al. 2012). In irregular echinoids, sympatry was observed between closely related species of the genus *Echinocardium* (between *Echinocardium cordatum* and *Echinocardium flavescens* in Norway, pers. obs.), as well as between species of the sand dollar *Mellita* along the tropical coasts of the Americas (Coppard et al. 2013). Sympatry between attested, cryptic species is much more rare. Examples are documented in the sand dollar *Mellita*, in which only one of nine possible cases of sympatry between cryptic species was recorded (Coppard et al. 2013), and in the species complex *E. cordatum* (Egea et al. 2011, 2016). Contrary to these two case studies, all species of *Abatus* are brooders and, consequently, show limited dispersal capability compared to sea urchins with planktonic larvae. The coexistence of *A. bidens* and *A. cavernosus* at the same sites (Fig. 3c) is therefore unexpected, all the more that previous studies revealed significant genetic differentiation between populations of *Abatus* species at small spatial scale such as in *A. cordatus* (Poulin and Féral 1995; Ledoux et al. 2012), *A. agassizi* (Díaz et al. 2012), and *A. nimrodi* (Chenuil et al. 2004). In the present case study, the mechanisms involved in the separation between the three forms cannot be uncovered with confidence. Morphological similarities do not support the hypothesis of a strict ecological mechanism at the origin of the divergence for the three groups, and the two forms of *A. bidens* in particular probably have similar modes of life. The separation is more likely rooted in life history traits (e.g., shifts in spawning seasons) or in prezygotic isolation (i.e., incompatibility between gamete recognition proteins) (Lessios 2011). Finally, it cannot be excluded that haplogroups of *A. bidens* may interbreed with no fitness cost and belong to the same biological species, nor that post-zygotic incompatibility only is involved in the isolation of the two forms despite the evolutionary cost it would imply.

At the scale of the three geographic areas explored, the two forms of *A. bidens* were not collected in the Drake Passage, while conversely, *A. cavernosus* was frequently found there (at 83 % of the sampling sites). The latter species is also present in the Bransfield Strait, but it was less frequently found than *A. bidens*, and it is absent from the northwest of the Weddell Sea (namely, no sequence of *A. cavernosus* was identified in the Weddell Sea) (Fig. 9). Two distinct distribution patterns seem to appear and to follow reverse, latitudinal gradients: *A. cavernosus* is the most frequently encountered to the north, and most often outside the areas strongly impacted by sea ice, while the two forms of *A. bidens* are the most frequent to the south in areas under sea ice influence (Fig. 9). Though still in need for further research, these apparent patterns are supported by records of *A. cavernosus* at the tip of South America (Bernasconi 1925, 1966) and by the putative presence of *A. bidens* in Adelie Land (Koehler (1926) described

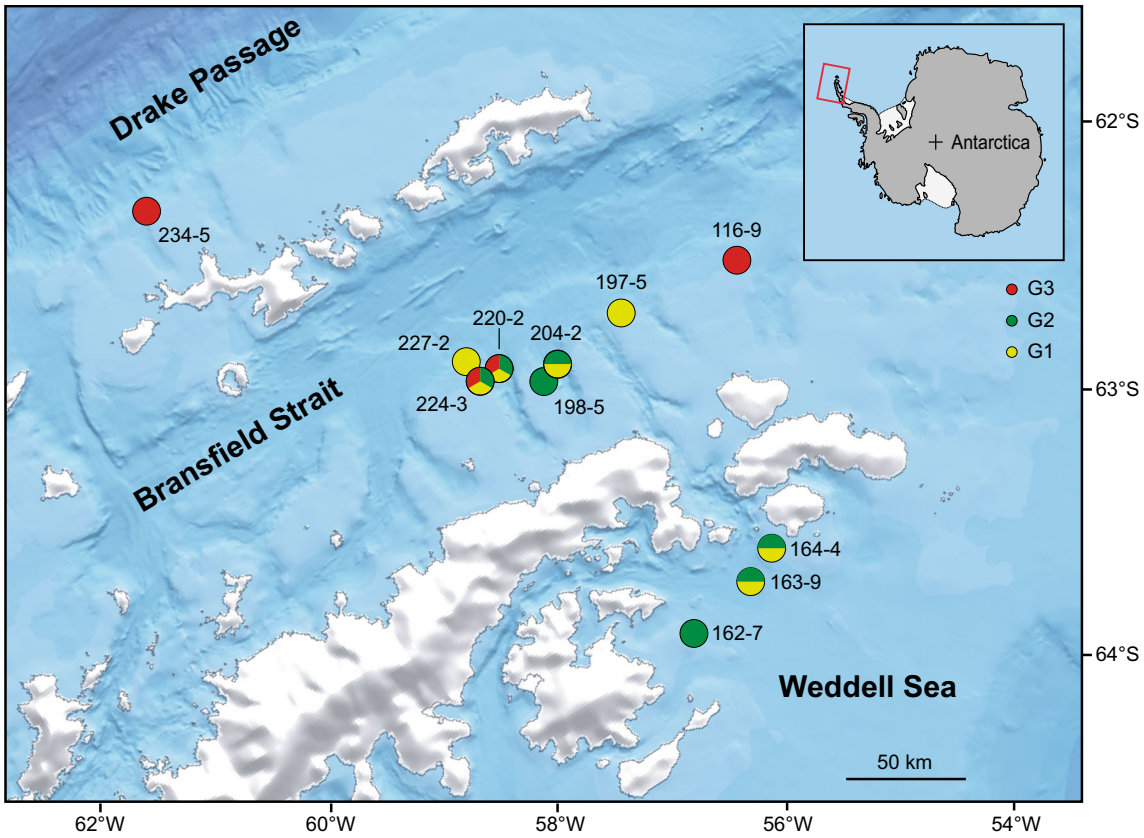


**Fig. 9** Distribution map of the genetic groups of *Abatus cavernosus* and *Abatus bidens* (G1 *light green*; G2 *dark green*; G3 *red*) among the 14 stations where they were identified. *Circle wedges* indicate the presence/absence of genetic groups, not abundance. (Color figure online)

globiferous pedicellariae of "*A. cavernosus*" with two long hooks, suggesting that its specimens should be regarded as *A. bidens*). The two species have been also unquestionably recognized to co-occur in South Georgia (Bernasconi 1953). This is not contradictory with the proposed pattern as South Georgia has been often regarded as a biogeographic area under the cross-influence of Antarctic and sub-Antarctic regions. Although unevenly distributed, the three haplogroups co-occur in the Bransfield Strait where they can be found in sympatry. Such a diversity pattern has already been highlighted in previous studies for other organisms (Wilson et al. 2007; Hemery et al. 2012). Along with the Scotia Arc region and the northern tip of the Antarctic Peninsula, the Bransfield Strait is a favored zone of connectivity among populations due to the strong current systems present near the tip of the Antarctic Peninsula (Thompson et al. 2009).

At the scale of the entire Southern Ocean, the attested occurrence of *A. bidens* in the peninsula area as well as in Adelie Land suggests that the species has a wide, potentially circumpolar distribution. The respective distribution of the two haplogroups still remains to be clarified, in East Antarctica in particular. In contrast, *A. cavernosus* seems to have a more northern distribution, potentially restricted to the Magellanic and Scotia Arc regions as no report of *A. cavernosus* outside this area is fully certain. This distribution pattern is in complete opposition with previous works (David et al. 2005a).

## Conclusion

Pending for further genetic analyses including closely related species of *Abatus* (i.e., *A. philippi*, *A. agassizi*, and *A. cordatus*) and additional samplings in other areas of the Southern Ocean, the present study, however, suggests that the *A. cavernosus–A. bidens* complex comprises at least two morphologically close species and two cryptic species. It contributes to clarifying the systematics of *A. cavernosus* and *A. bidens* and shows that *A. bidens* should definitely be regarded as distinct from *A. cavernosus*, based on congruent morphological characters and genetic results. In addition, *A. cavernosus* and the two forms of *A. bidens* were shown to have distinct distribution patterns.

The present work is also the first study to report the occurrence of putative cryptic species of echinoids in the Southern Ocean, in accordance with many observations of various marine invertebrates of the Southern Ocean. It

leads to revisit the richness of the Antarctic echinoid fauna, its systematics, and macroecological patterns, and to re-assess the underpinning evolutionary processes and history. It also highlights the crucial importance of associated morphological and genetic studies for improving our knowledge of Antarctic biodiversity. This is a prerequisite for further process-based studies, from ecology to phylogeography, and for uncovering the origin of the rich Antarctic biodiversity.

**Acknowledgments** Samples were collected during the oceanographic campaign PS81–ANT-XXIX/3 of the R/V *Polarstern*. The authors would like to thank Prof. Dr. Julian Gutt, chief scientist of this campaign, as well as the crew and the scientific staff. Chantal De Ridder was supported by F.R.S-FNRS "short stay abroad" travel grants (Grant Nr. 2013/V3/5/035). This is contribution nr. XX to the vERSO project (www.versoproject.be), funded by the Belgian Science Policy Office (BELSPO, Contract nr. BR/132/A1/vERSO, contribution n° 9). This is a contribution to team BioME of the CNRS laboratory Biogéosciences (UMR 6282).

**Compliance with ethical standards**

**Conflict of interest** The authors declare that they have no conflict of interest.

## References

Aguilée R, Claessen D, Lambert A (2012) Adaptive radiation driven by the interplay of eco-evolutionary and landscape dynamics. Evolution 67(5):1291–1306. doi:10.1111/evo.12008

Allcock AL, Strugnell JM (2012) Southern Ocean diversity: new paradigms from molecular ecology. Trends Ecol Evol 27:520–528

Allcock AL, Barratt I, Eléaume M, Linse K, Smith PJ, Steinke G, Stevens DW, Norman MD, Strugnell JM (2010) Cryptic speciation and the circumpolarity debate: a case study on endemic Southern Ocean octopuses using the COI barcode of life. Deep Sea Res II 58:242–249

Baird HP, Miller KJ , Stark JS (2011) Evidence of hidden biodiversity, ongoing speciation and diverse patterns of genetic structure in giant Antarctic amphipods. Mol Ecol 20:3439–3454

Bandelt HJ, Forster P, Röhl A (1999) Median-joining networks for inferring intraspecific phylogenies. Mol Biol Evol 16:37–48

Bernasconi I (1925) Resultados de la primera expedicion a Tierra del Fuego (1921). Echinodermos. I Equinoideos. Anales Soc Ci Argent 98:3–17

Bernasconi I (1953) Monografia de los equinoideos argentinos. Anales Mus Nac Hist Nat Buenos Aires 2(6):1–58

Bernasconi I (1966) Los equinoideos y asteroideos colectados por el buque oceanografico R/V "Vema", frente a las costas Argentinas, Uruguayas y sur de Chile. Revista Mus Argent Ci Nat "Bernardino Rivadavia" 9:147–175

Boissin E, Stöhr S, Chenuil A (2011) Did vicariance and adaptation drive cryptic speciation and evolution of brooding in *Ophioderma longicauda* (Echinodermata: Ophiuroidea), a common atlanto-mediterranean ophiuroid? Mol Ecol 20:4737–4755

Chenuil A, Féral JP (2003) Sequences of mitochondrial DNA suggest that *Echinocardium cordatum* is a complex of several sympatric or hybridizing species. A pilot study. In: Féral JP, David B (eds) Echinoderm Research 2001. Swets & Zeitlinger, Lisse, pp 15–21

Chenuil A, Gault A, Féral JP (2004) Paternity analysis in the Antarctic brooding sea urchin *Abatus nimrodi*. A pilot study. Polar Biol 27:117–182

Chenuil A, Egea E, Rocher C, Touzet H, Féral JP (2008) Does hybridization increase evolutionary rates? Data from the 28S-rDNA D8 domain in echinoderms. J Mol Evol 67:539–550

Chenuil A, Egea E, Rocher C, Féral JP (2010) Comparing substitution rates in spatangoid sea urchins with putatively different effective sizes, and other echinoderm datasets. In: Harris LG, Böttger SA, Walker CW, Lesser MP (eds) Echinoderms Durham. Balkema, Leiden, pp 159–161

Coppard S, Zigler KS, Lessios HA (2013) Phylogeography of the sand dollar genus *Mellita*: cryptic speciation along the coasts of the Americas. Mol Phylogenet Evol 69:1033–1042

David B, Mooi R (1990) An echinoid that "gives birth": morphology and systematics of a new Antartic species, *Urechinus mortenseni* (Echinodermata, Holasteroida). Zoomorphology 110:75–89

David B, Choné T, Mooi R, De Ridder C (2005a) Antarctic echinoidea. Synopses of the Antarctic Benthos. Koeltz Scientific Books, Königstein

David B, Choné T, Mooi R, De Ridder C (2005b) Biodiversity of Antarctic echinoids: a comprehensive and interactive database. Sci Mar 69:201–203

De Broyer C, Danis B et al (2011) How many species in the Southern Ocean? Towards a dynamic inventory of the antarctic marine species. Deep Sea Res II 58:5–17

Dettai A, Adamowizc SJ, Allcock L, Arango CP, Barnes DKA, Barratt I, Chenuil A, Couloux A et al (2011) DNA Barcoding and molecular systematics of the benthic and demersal organisms of the CEAMARC survey. Polar Sci 5:298–312

Díaz A, González-Wevar CA, Maturana CA, Palma AT, Poulin E, Gérard K (2012) Restricted geographic distribution and low genetic diversity of the brooding sea urchin *Abatus agassizii* (Spatangoidea: Schizasteridae) in the South Shetland Islands: a bridgehead population before the spread to the northern Antarctic Peninsula. Rev Chil Hist Nat 85:457–468

Egea E, Mérigot B, Mahé-Bézac C, Féral JP, Chenuil A (2011) Differential reproductive timing in *Echinocardium spp.*: the first Mediterranean survey allows inter-oceanic and inter-specific comparisons. C R Biol 334:13–23

Egea E, David B, Choné T, Laurin B, Féral JP, Chenuil A (2016) Morphological and genetic analyses reveal a cryptic species complex in the echinoid *Echinocardium cordatum* and rule out a stabilizing selection explanation. Mol Phylogenet Evol 94:207–220

Gutt J (2013) The expedition of the research vessel "Polarstern" to the Antarctic in 2013 (ANT-XXIX/3). Berichte zur Polar- und Meeresforsch 665:1–151

Hall TA (1999) BioEdit: a user-friendly biological sequence alignment editor and analysis program for Windows 95/98/NT. Nucleic Acids Symp Ser 41:95–98

Hammer Ø, Harper DAT, Ryan PD (2001) PAST: paleontological Statistics Software Package for education and data analysis. Pal Elec 4(1):1–9

Held C (2001) No evidence for slow-down of molecular substitution rates at subzero temperatures in Antarctic serolid isopods(Crustacea, Isopoda, Serolidae). Polar Biol 24:497–501

Held C, Wägele JW (2005) Cryptic speciation in the giant Antarctic isopod *Glyptonotus antarcticus* (Isopoda: Valvifera: Chaetiliidae). Sci Mar 69(2):175–181

Hemery LG, Eléaume M, Roussel V, Améziane N, Gallut C, Steinke D, Cruaud C, Couloux A, Wilson NG (2012) Comprehensive sampling reveals circumpolarity and sympatry in seven mitochondrial lineages of the Southern Ocean crinoid species *Promachocrinus kerguelensis* (Echinodermata). Mol Ecol 21:2502–2518

Hoareau TB, Boissin E (2010) Design of phylum-specific hybrid primers for DNA barcoding: addressing the need for efficient COI amplification in the Echinodermata. Mol Ecol Res 10:960–967

Kaiser S, Brandão SN, Brix S, Barnes DKA, Bowden DA, David B, Gutt J et al (2013) Pattern, process and vulnerability of Antarctic and Southern Ocean benthos: a decadal leap in knowledge and understanding. Mar Biol 160:2295–2317

Koehler R (1912) Echinodermes nouveaux recueillis dans les mers antarctiques par le Pourquoi-pas (astéries, ophiures et échinides). Zool Anz 39:151–163

Koehler R (1926) Echinodermata Echinoidea. Australasian Antarctic expedition 1911–1914. Sci Rep 8:1–134

Krabbe K, Leese F, Mayer C, Tollrian R, Held C (2009) Cryptic mitochondrial lineages in the widespread pycnogonid *Colossendeis megalonyx* Hoek, 1881 from Antarctic and Subantarctic waters. Polar Biol 33:281–292

Kroh A (2015) *Abatus cavernosus bidens* Mortensen, 1910. In: Kroh A, Mooi R (eds) World Echinoidea Database. Accessed through: World Register of Marine Species

Lecointre G, Améziane N, Boisselier MC, Bonillo C, Busson F, Causse R, Chenuil A, Couloux A et al (2013) Is the species flock concept operational? The Antarctic Shelf Case. PloS One 8:e68787

Ledoux JB, Tarnowska K, Gérard K, Lhuillier E, Jacquemin B, Veydmann A, Féral JP, Chenuil A (2012) Fine-scale spatial genetic structure in the brooding sea urchin *Abatus cordatus* suggests vulnerability of the Southern Ocean marine invertebrates facing global change. Polar Biol 35:611–623

Lessios HA (2011) Speciation genes in free-spawning marine invertebrates. Integr Comp Biol 51:456–465

Linse K, Cope T, Lörz AN, Sands C (2007) Is the Scotia Sea a centre of Antarctic marine diversification? Some evidence of cryptic speciation in the circum-Antarctic bivalve *Lissarca notorcadensis* (Arcoidea: Philobryidae). Polar Biol 30:1059–1068

Mortensen T (1909) Die Echinoiden der Deutschen Südpolar Expedition 1901-1903. Deutsche Südpolar Expedition. G Reimer, Berlin

Mortensen T (1910) The Echinoidea of the Swedish South Polar Expedition. Wissenschaftliche Ergebnisse der Schwedischen Südpolar-Expedition 1901–1903. Lithographisches Institut des Generalstabs, Stockholm

Mortensen T (1951) A monograph of the Echinoidea. Vol. 5.2 Spatangoida II. Reitzel CA, Copenhagen

Néraudeau D, David B, Madon C (1998) Tuberculation in spatangoid fascioles: delineating plausible homologies. Lethaia 31:323–334

O'Loughlin PM, Paulay G, Davey N, Michonneau F (2011) The Antarctic region as a marine biodiversity hotspot for echinoderms: diversity and diversification of sea cucumbers. Deep Sea Res II 58:264–275

Pawson DL (1969) Echinoidea. In: Bushnell VC, Hedgpeth JW (eds) Distribution of selected groups of marine invertebrates in water south of 35°S latitude. Antarctic map folio. Am Geogr Soc, New York, p 38–41

Pearse J, Mooi R, Lockhart SJ, Brandt A (2009) Brooding and species diversity in the southern ocean: selection for brooders or speciation within brooding clades? In: Krupnik I, Lang MA, Miller SE (eds) Smithsonian at the poles: contributions to international polar year science. Smithsonian Institution Scholarly Press, Washington, pp 181–196

Pierrat B, Saucède T, Festeau A, David B (2012) Antarctic, sub-Antarctic and cold temperate echinoid database. ZooKeys 204:47–52. doi:10.3897/zookeys.204.3134

Poulin E, Féral J-P (1995) Pattern of spatial distribution of a brood-protecting Schizasterid Echinoid, Abatus cordatus, endemic to Kerguelen Islands. Mar Ecol Prog Ser 118:179–186

Poulin E, Palma AT, Féral J-P (2002) Evolutionary versus ecological success in Antarctic benthic invertebrates. Trends Ecol Evol 17:218–222

Raupach MJ, Wägele JW (2006) Distinguishing cryptic species in Antarctic Asellota (Crustacea: Isopoda): a preliminary study of mitochondrial DNA in *Acanthaspidia drygalskii*. Antarct Sci 18:191–198

Saucède T, Pierrat B, David B (2014) Chapter 5.26 Echinoids. In: De Broyer C, Koubbi P, Griffiths HJ, Raymond B, d'Udekem d'Acoz C et al (eds) Biogeographic atlas of the Southern Ocean. Scientific Committee on Antarctic Research, Cambridge, p 213–220

Schüller M (2011) Evidence for a role of bathymetry and emergence in speciation in the genus *Glycera* (Glyceridae, Polychaeta) from the deep Eastern Weddell Sea. Polar Biol 34:549–564

Smith PJ, Steinke D, McMillan PJ, Stewart AL, McVeagh SM, Diaz de Astarloa JM, Welsford D, Ward RD (2011) DNA barcoding highlights a cryptic species of grenadier *Macrourus* in the Southern Ocean. J Fish Biol 78:355–365

Statsoft France (2002) STATISTICA (logiciel d'analyse de données). Versio 6, www.Statsoft.com

Stockley B, Smith AB, Liittlewood T, Lessios HA, Mackenzie-Dodds JA (2005) Phylogenetic relationships of spatangoid sea urchins (Echinoidea): taxon sampling density and congruence between morphological and molecular estimates. Zool Scr 34:447–468

Thatje S, Hillenbrand C, Larter R (2005) On the origin of Antarctic marine benthic community structure. Trends Ecol Evol 20:534–540

Thompson AF, Heywood KJ, Thorpe SE, Renner AHH, Trasvina A (2009) Surface circulation at the tip of the Antarctic Peninsula from drifters. J Phys Oceanogr 39:3–26

Ward RD, Holmes BH, O'Hara TD (2008) DNA barcoding discriminates echinoderm species. Mol Ecol Res 8:1202–1211

Wilson NG, Hunter RL, Lockhart SJ, Halanych KM (2007) Multiple lineages and absence of panmixia in the "circumpolar" crinoid *Promachocrinus kerguelensis* from the Atlantic sector of Antarctica. Mar Biol 152:895–904

Wilson NG, Maschek A, Baker BJ (2013) A species flock driven by predation? Secondary metabolites support diversification of slugs in Antarctica. PLoS One 8:e80277